



## Report from

Matthew Pepper,  
Li Wang,  
Ajay Padmakumar,  
Timothy C. Burg,  
Sarah W. Harcum,  
Richard E. Groff,  
Department of Electrical and  
Computer  
Engineering/Department of  
Bioengineering, Clemson  
University



## A Real-time Adaptive Oxygen Transfer Rate Estimator for Metabolism Tracking in *Escherichia coli* cultures

### Introduction

Oxygen and carbon dioxide off-gas measurement enables the application of advanced estimation and control methods for aerobic bioprocesses. BlueSens, GmbH (Herten, Germany) offers an exhaust gas sensor capable of measuring mole ratios of both oxygen and carbon dioxide with accuracy comparable to mass spectrometry, the benchmark standard, but at a fraction of the cost [1]. The reduced cost makes it feasible to dedicate a sensor to each bioreactor to enable more sophisticated real-time estimation and control of bioprocesses. Direct computation of the oxygen transfer rate (OTR) from any type of off-gas measurement is problematic for use in control, since transport dynamics and sensor dynamics cause the computed OTR to be an attenuated and delayed version of the true OTR signal. The primary objective of this report is to describe a state estimator that combines exhaust gas, stir speed, and dissolved oxygen measurements to predict the true OTR in real time without attenuation or delay. The predicted OTR can be used for a variety of controls and estimation purposes, such as determining when the culture is in oxidative or overflow metabolism.

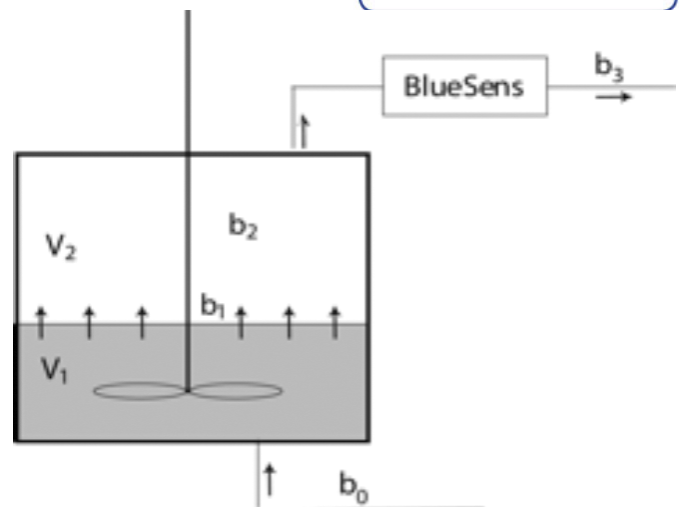


Figure 1 – Oxygen concentration in a stirred-tank bioreactor, the input gas concentration is  $b_0$ , the concentration exiting the liquid,  $b_1$ , the concentration of the head-space  $b_2$ , and  $b_3$  the concentration reported by the sensor.

### Background: OTR Dynamics

In a stirred-tank bioreactor, the input gas passes through two stages before being measured by the exhaust gas sensor. Figure 1 shows a bioreactor and attached off-gas sensor. The input gas contains a known concentration of oxygen,  $b_0$ . The gas enters

from the bottom of the vessel and a rotating impeller breaks up the bubbles, facilitating the absorption of oxygen into the culture. The difference in oxygen concentration between the entering gas,  $b_0$ , and the exiting gas,  $b_1$ , represents the amount of oxygen transferred into the liquid  $V_1$ . Assuming the mass inflow is equal to the outflow, this difference can be used to calculate the OTR in the liquid,

$$\text{OTR} = \frac{M_f(b_0 - b_1)\rho_{O_2}}{V_1} \quad (1)$$

where  $M_f$  is the mass flow,  $\rho_{O_2}$  is the density of oxygen at 25°C, and  $V_1$  is the volume of the liquid. OTR can also be modeled using the stir speed and dissolved oxygen concentration,

$$\begin{aligned} \text{OTR} &= k_L a (C^* - C) \\ k_L a &= \alpha_0 + \alpha_1 (N - N_0) \end{aligned} \quad (2)$$

where  $k_L a$  is the oxygen transfer coefficient,  $C^*$  is the maximum oxygen carrying capacity of the liquid,  $C$  is the current dissolved oxygen concentration, and  $N$  is stir speed. The dependence of  $k_L a$  on stir speed  $N$  is modeled as linear about stir speed  $N_0$ .

The gas leaving  $V_1$  mixes with the gas in the headspace volume  $V_2$ , resulting in the oxygen concentration  $b_1$ . This process is a standard mixing model,

$$\dot{b}_2 = \frac{M_f}{V_2} (b_1 - b_2) \quad , (3)$$

where  $M_f$  is the mass flow rate. The concentration  $b_2$  is sampled by the BlueInOne sensor, and the sensor output,  $b_3$ , is modeled as a first order linear system with time constant  $\tau_2$ ,

$$\dot{b}_3 = \frac{1}{\tau_2} (b_2 - b_3) \quad . (4)$$

Clearly, computing OTR directly from the concentration  $b_3$  would be significantly different from the true value of OTR computed from concentration  $b_1$ .

## Estimator Design

A state estimator predicts the unmeasurable state variables of a system by using the measureable

outputs and inputs in combination with the known dynamics of the system. When an adaptive state observer is used, the system dynamics are known except for some unknown or time-varying parameters. In the bioreactor system presented in the previous section, the oxygen concentration dynamics are represented by the state variables  $b_2$  and  $b_3$ , which follow the dynamics given by Eqns (3) and (4). The input to the system is concentration  $b_1$ , which cannot be measured directly, but can be computed from stir speed using Eqns (1) and (2),

$$b_1 = b_0 - \frac{V_1(C^* - C)}{M_f \rho_{O_2}} \alpha_0 - \frac{V_1(C^* - C)(N - N_0)}{M_f \rho_{O_2}} \alpha_1 \quad . (5)$$

All parameters in the model may be reliably characterized in advance, with the exception of the parameters  $\alpha_0$  and  $\alpha_1$  which relate stir speed to  $k_L a$ . These parameters are notoriously hard to find and tend to vary slowly over the length of the culture [2,4]. The estimator described in this report uses an adaptive law based on measurements from the BlueSens sensor to identify the possibly-time-varying parameters  $\alpha_0$  and  $\alpha_1$  in real time. With good estimates of these parameters, OTR can be accurately predicted from stir speed and dissolved oxygen concentration using Eqn (2).

## Estimator Mathematics

The adaptive estimator is based on a structure from [6]. The mathematics for the estimator will be briefly summarized. The estimator is based on the sensor and transport dynamics, Eqns (3) to (5), rewritten as a state space model in observable canonical form,

$$\begin{aligned} \dot{x} &= Ax + Bf \\ y &= Cx, \\ A &= \begin{bmatrix} -\frac{M_f}{V_2} - \frac{1}{\tau_2} & 1 \\ -\frac{M_f}{V_2\tau_2} & 0 \end{bmatrix}, B = \begin{bmatrix} 0 & 0 & 0 \\ \frac{\alpha_0}{\tau_2} & \frac{\alpha_1}{\tau_2} & \frac{b_0}{\tau_2} \end{bmatrix}, C = \begin{bmatrix} 1 & 0 \end{bmatrix} \\ f &= \begin{bmatrix} f_0 \\ f_1 \\ f_2 \end{bmatrix} = \begin{bmatrix} -\frac{V_1(C^* - C)}{V_2\rho_{O_2}} \\ -\frac{V_1(C^* - C)(N - N_0)}{V_2\rho_{O_2}} \\ \frac{M_f}{V_2} \end{bmatrix} \end{aligned} \quad (6)$$

The adaptive estimator simultaneously estimates the state variables  $b_2$  and  $b_3$  and the parameters  $a_0$  and  $a_1$ . The estimator is driven by known variables  $b_3$ ,  $C$ ,  $N$ ,  $V_1$ , and  $V_2$ . The adaptive estimator is given by

$$\begin{aligned} \dot{\hat{x}} &= A\hat{x} + \begin{bmatrix} 0 \\ \hat{\alpha}_0 \end{bmatrix} \frac{f_0}{\tau_2} + \begin{bmatrix} 0 \\ \hat{\alpha}_1 \end{bmatrix} \frac{f_1}{\tau_2} + \begin{bmatrix} 0 \\ b_0 \end{bmatrix} \frac{M_f}{V_2\tau_2} + v_0 + v_1 \\ \dot{e} &= Ae + \phi_0 \frac{f_0}{\tau_2} + \phi_1 \frac{f_1}{\tau_2} + v_0 + v_1 \\ e_1 &= Ce \\ v_0^T &= -\phi_0^T \begin{bmatrix} 0 & -\frac{4f_0}{\tau_2(s+4)} \\ 0 & \frac{4f_0}{\tau_2(s+4)} \end{bmatrix} v_1^T = -\phi_1^T \begin{bmatrix} 0 & -\frac{4f_1}{\tau_2(s+4)} \\ 0 & \frac{4f_1}{\tau_2(s+4)} \end{bmatrix} \end{aligned} \quad (7)$$

where  $e = \hat{x} - x$ ,  $e_1 = \hat{y} - y$ ,  $\phi_0 = [0 \quad \hat{\alpha}_0 - \alpha_0]^T$ ,  $\phi_1 = [0 \quad \hat{\alpha}_1 - \alpha_1]^T$ .  $v_0$  and  $v_1$  are auxiliary variables. The adaptive law for the two unknown parameters are designed as  $\dot{\hat{\phi}}_0 = -\gamma_0 e_1 \omega_0$ ,  $\dot{\hat{\phi}}_1 = -\gamma_1 e_1 \omega_1$  where  $g_0$  and  $g_1$  are observer gains. Other variables are designed as

$$\omega_0 = \begin{bmatrix} \frac{s}{s+4} & \frac{1}{s+4} \end{bmatrix} \frac{f_0(t)}{\tau_2}, \omega_1 = \begin{bmatrix} \frac{s}{s+4} & \frac{1}{s+4} \end{bmatrix} \frac{f_1(t)}{\tau_2}$$

Note that the argument  $s$  denotes the differential operator  $d/dt$ .

Table 1 contains all the parameters for the oxygen dynamics model.  $k_L a$  is known to slowly change over the course of a fermentation and is influenced by multiple factors such as anti-foam addition and liquid viscosity changes; therefore, the values for the linear model seen in Eqn. (2) are time-varying and can only be defined approximately.

Parameter	Name	Value
$M_f$	Mass Flow rate	3 L/min
$V_3$	Culture volume	1.67 L
$V_4$	Headspace volume	5.03 L
$\tau_4$	BlueSens time constant	55 s
$\rho_{O_4}$	Oxygen density	1.331 g/L
$\alpha_2$	Initial value	0.0035 1/s
$\alpha_3$	Initial value	0.00022 1/(s·RPM)
$b_2$	Input Oxygen Volume	20.97%
$C^*$	Maximum Oxygen carrying capacity	6.71 mg/L
$N_2$	Initial Stir speed	200 RPM

Table 1: Adaptive Estimator Parameters

## Experiments

### Bioreactor System

The bioreactor system is a Sartorius Biostat B 5-L glass vessel and digital control unit (DCU). The DCU connects to probes for pH (Hamilton Company, Reno, NV), temperature (Sartorius AG), and dissolved oxygen (Hamilton). The data is sampled every 15 seconds using the OPC protocol in a Simulink model running on Matlab 2012a (Mathworks Inc. Natick, MA). The model also samples the relative humidity, temperature, pressure, and oxygen and carbon dioxide volumetric percentages coming from the BlueSens BlueInOne exhaust gas analyzer every 10 seconds. The mass flow of the sparged gas is measured with a mass flow controller (Omega Engineering Inc, Stamford, CT) and sampled every 5 seconds. Lastly, two balances (Ohaus Corp, Parsippany, NJ) keep track of the amount of glucose and base dispensed and report weight every 5 seconds.

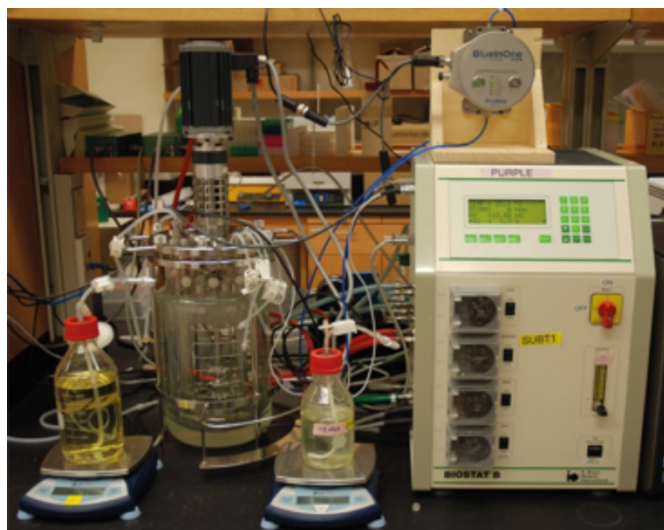


Figure 2 – The Biostat-B bioreactor system, shown with 5 L vessel and motor, DCU, BlueSens BlueInOne sensor, and Balances.

## Sensor Characterization

In order to implement the adaptive OTR estimator on the system, the behavior of the BlueInOne sensor was analyzed in several characterization experiments. The first experiment was a study of the delay and response time of the sensor,  $t_d$ . Previous publications have numbers for response time and measurement delay, but for a different model and at a much smaller flow rate (0.040 vs. 2 L/min (lpm)). The input gas,  $bo$ , was connected directly to the input of the BlueInOne sensor, bypassing the stirred-tank vessel; this allowed for measurement of only the sensor dynamics. In this experiment, the composition and flow of the input gas was varied. The input gas was switched from nitrogen to air in 5 minute increments. The gas would cycle twice, and then the flow rate would increase by 1 lpm, from 2 to 8 lpm. The delay (15 seconds) represents the time it took the sensor to respond once the gas composition had changed. The response time (55 seconds) is the time constant for the sensor, i.e., the time for the sensor to reach 63% of its final value. The data showed that the response time did not change with increasing gas flow, indicating the measuring chamber in the BlueInOne was being flushed well above maximum requirements.

The second experiment explored the accuracy and stability of the sensor measurements to changes in pressure, ranging from 1.02 to 1.67 bar. This experiment determined the usability of the sensor in experiments requiring pressurizing of the headspace. The Biostat-B vessel has a maximum pressure limit of 1.63 bar. The manufacturer's certified, accurate operational pressure range for the BlueInOne sensor is between 0.8 and 1.3 bar, with a maximum of 2 bar. The experiment began by performing a one-point calibration on the BlueInOne; the input gas of air had a constant assumed oxygen volume of 20.97%. As in the previous experiment, the input gas was connected directly to the input port of the BlueInOne sensor. The mass flow rate was varied between 1 and 9 lpm in steps of 1 lpm. The steps in mass flow caused the internal pressure of the sensor to rise from 1 to 1.67 bar (Table 2).

Mass Flow (lpm)	Pressure (bar)	Pressure Step (bar)	O <sub>2</sub> Volume (%)	O <sub>2</sub> Spike (%)	O <sub>2</sub> Spike Duration (s)
1	1.02		20.97		
2	1.06	0.045	20.97	1.35	35
3	1.12	0.055	20.97	1.85	45
4	1.18	0.064	20.96	2.41	75
5	1.27	0.081	20.97	3.17	55
6	1.35	0.085	20.98	3.53	85
7	1.45	0.095	21.01	3.78	55
8	1.56	0.105	21.04	3.57	75
9	1.67	0.110	21.10	3.49	85

Table 2: Measurement Stability Tests

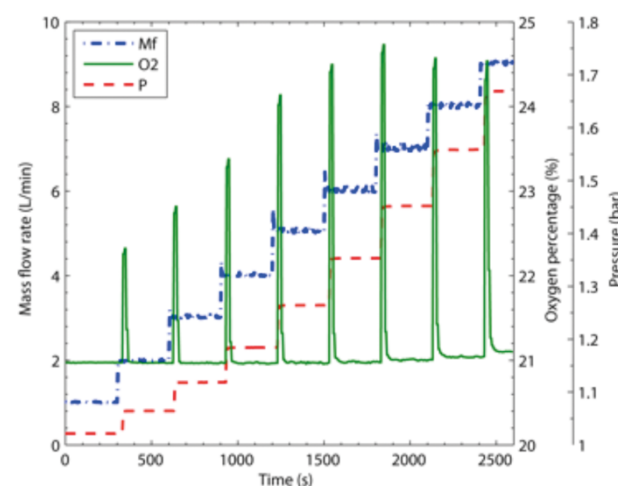


Figure 3 – Measurement Stability Results, the pressure compensation algorithm in the BlueInOne quickly



corrected any error caused by the step changes in pressure. The final corrected value changed by less than 1% over the tested pressure range.

After each step of the flow rate and pressure, the reading would spike due to the increased amount of oxygen in the chamber. The compensation software acted quickly to correct the reported measurement, and on average only 64 ( $\pm 19$ ) seconds of data was affected. The reported oxygen volume drifted from 20.97% to 21.1% over this range of pressure, representing <1% error. As expected, the base reading began to drift above 1.3 bar. The pressure compensation software produced accurate measurements even outside its certified range, indicating the sensor should yield accurate stable readings under conditions of constant or slowly varying pressure.

### Bioreactor Conditions

Two experiments were performed to test the accuracy of the OTR estimator. In the first experiment, the OTR estimator was implemented on a bioreactor simulator. The delays on input and output data characteristics mirror that of the Sartorius Biostat-B, the BlueInOne sensor, and the two balances. The simulated behavior of the *Escherichia coli* (*E. coli*) is based on the work of 1999 Xu [8]. In the second experiment, *E. coli* MG1655 pTV1GFP [5] was cultured for 12 hours in minimal media. The bioreactor was inoculated at an optical density (measured by spectrophotometer) of 0.5 OD. In both experiments, the growth rate was kept at 0.25 h<sup>-1</sup>. The volume of the culture was 1.67 L. The mass flow of the input gas was 3 liters per minutes.

### Validation of the OTR Estimator

A feed rate disturbance in the form of a pulse was used to test the capability of the OTR estimator to track *E. coli* metabolism. The pulse increased the feed rate to four times the current feed rate. This pulse was designed to increase the glucose concentration such that the *E. coli* enter overflow metabolism. While overflow metabolism is not desirable for *E. coli*, the

feed rate pulse is short and any negative byproduct is quickly consumed. Tracking the *E. coli* metabolism transition from oxidative to overflow will help determine a feed rate to keep the culture on the verge of overflow, maximizing oxidative metabolism.

In Figure 4, the experimental results (A, B) show the OTR and OUR rise sharply as the *E. coli* metabolism increased in response to the glucose pulse. This behavior duplicates the behavior seen in simulation, Figure 4 D and E, indicating that experimental results are reasonable. Notice the response of the OTR formed from the BlueInOne measurements, OTR<sub>sens</sub>. The filtering effects are seen in the attenuation of the maximum height of OTR<sub>sens</sub> versus the OTR<sub>est</sub> and the delay between both their respective peaks.

The response of the OTR<sub>est</sub> is almost immediate while the peak in OTR<sub>sens</sub> does not occur until after the 5 minute pulse is over. The plateau effect seen in OTR<sub>est</sub> indicates that the culture entered overflow metabolism. In overflow metabolism, the oxidative metabolism becomes saturated with glucose and any excess glucose absorbed by the cells is anaerobically converted to acetate, which can inhibit growth at high concentrations (2 g/L). The profile of OTR<sub>est</sub> indicates that the oxidative metabolism could process glucose at a higher rate, thus the feed rate could be increased significantly. A much longer pulse would be required to obtain the same data from OTR<sub>sens</sub>, resulting in significantly more acetate production.

The behavior of the *E. coli* in actual and simulated experiments was very similar, validating the tuning of the OTR estimator gains (Figure 4 A, B, D, and E). In the simulated experiments (Figure 4 D, E), the OTR<sub>est</sub> tracks the actual OTR very well. This indicates that the estimate of the  $k_L a$  parameters  $a_0$  and  $a_1$  converged to their true values. The  $k_L a$  for the actual fermentation was plotted in Figure 5. The distribution of the data points indicates the  $k_L a$  varied linearly with stir speed, validating our linear model. A linear model is appropriate since the short culture length did not allow the cell density to affect the viscosity of the media.

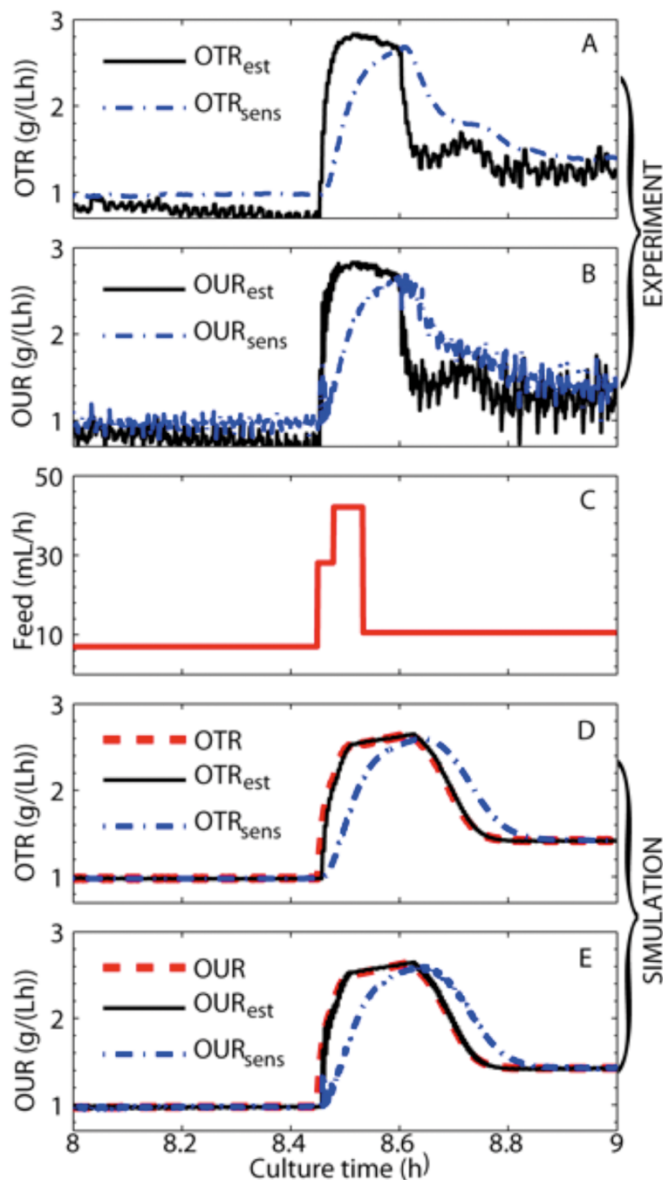


Figure 4 – Glucose Pulse Experiments, a pulse (C) in the feed rate was implemented to test tracking of the OTR estimator on actual (A, B) and simulated (D, E) bioreactor systems. In A, the OTR estimator was able to accurately track the OTR and provided a better indication of *E. coli* metabolism than the OTR using the BlueInOne measurements. The attenuation and delay effects of the system are clearly seen (A, B).

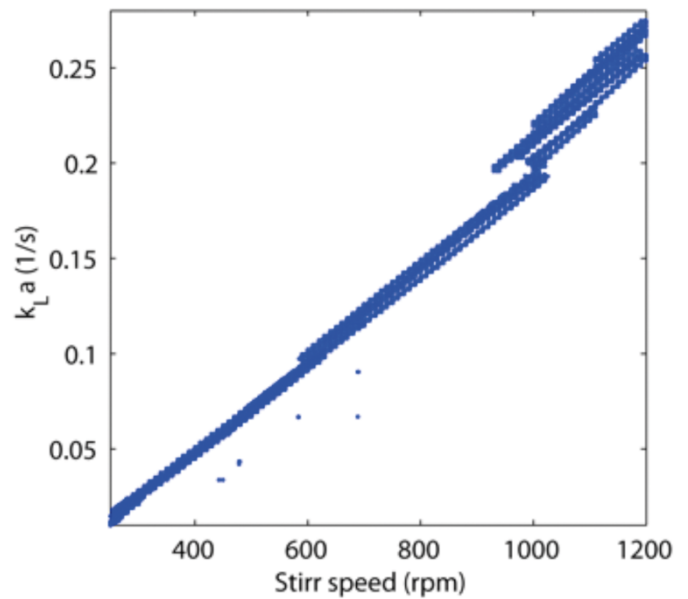


Figure 5 – Experimental Oxygen Transfer Coefficient, the estimates for the  $k_La$  calculated by the OTR estimator. The  $k_La$  and stirr speed maintained an approximately linear relationship during the 12 hour fermentation. This result validates the  $k_La$  model.

## Conclusions

The OTR estimator provided a more accurate OTR profile by removing the influences of the headspace and sensor dynamics on the exhaust gas oxygen volume measurement. The BlueInOne measurements provided both accurate and stable measurements, allowing the adaptive algorithm to estimate both the unknown  $k_La$  and OTR values. The OTR estimator accurately tracked the *E. coli* metabolism and will be an integral part in the development of maximizing controllers for oxidative metabolism and improving biomass yield.

Researchers have been using exhaust gas sensors to develop advanced estimator and control algorithms for over 20 years. The implementation of these advanced estimator and control algorithms in an industrial context has been very slow, much to the detriment of the industry [7]. Ranging from neural networks to model predictive control, the BlueInOne sensor enables academic and industrial researchers to explore and implement the next level of bioprocess control techniques.

## References

[1]

M. Aehle, R. Simutis, and A. Lubbert, "Comparison of viable cell concentration estimation methods for a mammalian cell cultivation process," *Cytotechnology*, vol. 62, no. 5, pp. 413–422, Oct 2010.

[2]

M. Akesson, P. Hagander, and J. P. Axelsson, "A pulse technique for control of fed-batch fermentations," in *Proceedings of the 1997 IEEE International Conference on Control Applications*, pp. 139–144.

[3]

V. Babaeipour, S. A. Shojaosadati, S. M. Robotjazi, R. Khalilzadeh, and N. Maghsoudi, "Over-production of human interferon by hcdc of recombinant *Escherichia coli*," *Process Biochemistry*, vol. 42, no. 1, pp. 112–117, Jan 2007.

[4]

G. Bastin and D. Dochain, *On-line Estimation and Adaptive Control of Bioreactors*. Amsterdam, Netherlands: Elsevier Science, 1990.

[5]

E. Garcia-Fruitos et al., "Aggregation as bacterial inclusion bodies does not imply inactivation of enzymes and fluorescent proteins," *Microb. Cell Fact.* vol. 4, no. 27.

[6]

K. S. Narendra, A. M. Annaswamy, *Stable Adaptive Systems*, Chp 4, Prentice Hall, Englewood Cliffs, NJ, 1989.

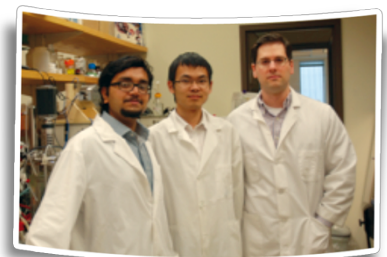
[7]

U. S. Food and D. A. (USFDA), "Guidance for industry process analytical technology (PAT) - a framework for innovative pharmaceutical development, manufacturing, and quality assurance," Sep 2004.

[8]

B. Xu, M. Jahic, and S. O. Enfors, "Modeling of overflow metabolism in batch and fed-batch cultures of *Escherichia coli*," *Biotechnology progress*, vol. 15, no. 1, pp. 81–90, Jan-Feb 1999.

The Cell-Culture and Optimization Lab is part of the Department of Bioengineering (BioE) at Clemson University under the direction of Sarah Harcum (harcum@clemson.edu). The work presented is in collaboration the Bio-Inspired Systems Lab in the Electrical and Computer Engineering (ECE) Department at Clemson University under the direction of Richard E. Groff (regroff@clemson.edu). The goal of this project is to develop advanced estimation and control strategies for the fermentation and culture of bacteria and mammalian cells. The research is supported by National Institute of Health (NIH) Centers of Biomedical Research Excellence (COBRE) under grant # P20GM103444.



## Project Team

Matthew E. Pepper (right)	PhD Student, ECE
Li Wang (center)	MS Student, ECE
Ajay Padmakumar (left)	MS Student, ECE
Dr. Timothy C. Burg	Associate Professor, ECE
Dr. Sarah W. Harcum	Associate Professor, BioE
Dr. Richard E. Groff	Associate Professor, ECE